Mon. Not. R. Astron. Soc. **363,** 609–614 (2005) doi:10.1111/j.1365-2966.2005.09465.x

High-speed, multicolour optical photometry of the anomalous X-ray pulsar 4U 0142+61 with ULTRACAM

V. S. Dhillon,[1⋆] T. R. Marsh,[2] F. Hulleman,[3] M. H. van Kerkwijk,[3,4] A. Shearer,[5] S. P. Littlefair,[1] F. P. Gavriil[6] and V. M. Kaspi[6]

[1]*Department of Physics and Astronomy, University of Sheffield, Sheffield S3 7RH*
[2]*Department of Physics, University of Warwick, Coventry CV4 7AL*
[3]*Astronomical Institute, Utrecht University, PO Box 80000, 3508 TA Utrecht, the Netherlands*
[4]*Department of Astronomy and Astrophysics, University of Toronto, 60 St. George Street, Toronto, Ontario, M5S 3H8, Canada*
[5]*Computational Astrophysics Group, Department of Information Technology, National University of Ireland, Galway, Ireland*
[6]*Department of Physics, Rutherford Physics Building, McGill University, 3600 University Street, Montreal, Quebec, H3A 2T8, Canada*

Accepted 2005 July 23. Received 2005 July 7; in original form 2005 May 26

ABSTRACT

We present high-speed, multicolour optical photometry of the anomalous X-ray pulsar 4U 0142+61, obtained with ULTRACAM on the 4.2-m William Herschel Telescope. We detect 4U 0142+61 at magnitudes of $i' = 23.7 \pm 0.1$, $g' = 27.2 \pm 0.2$ and $u' > 25.8$, consistent with the magnitudes found recently by Hulleman et al. and hence confirming their discovery of both a spectral break in the optical and a lack of long-term optical variability. We also confirm the earlier discovery of Kern & Martin that 4U 0142+61 shows optical pulsations with an identical period (∼8.7 s) to the X-ray pulsations. The rms pulsed fraction in our data is 29 ± 8 per cent, 5–7 times greater than the 0.2–8 keV X-ray rms pulsed fraction. The optical and X-ray pulse profiles show similar morphologies and appear to be approximately in phase with each other, the former lagging the latter by only 0.04 ± 0.02 cycles. In conjunction with the constraints imposed by X-ray observations, the results presented here favour a magnetar interpretation for the anomalous X-ray pulsars.

Key words: stars: neutron – pulsars: individual: 4U 0142+61.

1 INTRODUCTION

More than 100 X-ray pulsars are currently known. The vast majority of these are found in low-mass and high-mass X-ray binaries (LMXBs and HMXBs), and are hence powered by accretion on to a rotating, magnetized neutron star. There exists a small group of eight X-ray pulsars, however, that exhibit properties very much at variance with those of the accreting pulsars in X-ray binaries. These so-called anomalous X-ray pulsars (AXPs) all have ∼5–12 s spin periods, which decrease steadily with time, soft (and relatively low-luminosity) X-ray spectra, no radio emission, and tend to be associated with supernova remnants in the Galactic plane. Most importantly, the AXPs show no evidence of a binary companion. For a recent review of AXPs, see Woods & Thompson (2005).

This latter fact prompted a variety of models based on isolated neutron stars and white dwarfs (see the review by Israel, Mereghetti & Stella 2002), but these run into difficulty on energetic grounds: the loss of rotational energy, which powers radio pulsars like the Crab, is orders of magnitude too small to power the observed X-ray luminosity of the AXPs. An additional energy source is therefore required, for which two competing models seem to have emerged: accretion from a fossil disc or ultra-strong magnetic fields. In the former scenario, an isolated neutron star accretes from a fossil disc, such as might be produced through fall-back of material after a supernova explosion or left over from a common-envelope phase that destroyed the companion star. In the latter scenario, AXPs are 'magnetars', isolated neutron stars with enormous ($B \sim 10^{14}$–10^{15} G) magnetic fields. It is the decay of the magnetic field that heats the neutron star surface, causing it to emit thermal radiation in the X-rays. Non-thermal emission is then produced by particles accelerated in the magnetosphere by the Alfvén waves from small-scale fractures on the neutron star surface (Thompson & Duncan 1996) or Comptonization of thermal photons by magnetospheric currents (Thompson, Lyutikov & Kulkarni 2002).

The magnetar model has begun to dominate the literature in recent years. There are sound theoretical reasons for why this is so, as the magnetar model now appears to be able to explain the observational properties of several categories of supposedly young neutron stars that are not powered by rotation, including the AXPs and the soft gamma repeaters (SGRs). Such unification is supported by the recent discovery of SGR-like bursts in AXPs (Gavriil, Kaspi & Woods

⋆E-mail: vik.dhillon@shef.ac.uk

2002; Kaspi et al. 2003), which suggests that there might be an evolutionary link between AXPs and SGRs (see Mereghetti et al. 2002, and references therein).

What other observational evidence is there to support the magnetar model of AXPs? Belief in the magnetar model rests partly on the failure of the accretion model to explain the faintness of the optical/infrared counterparts, which sets strong limits on the size of an accretion disc (e.g. Hulleman, van Kerkwijk & Kulkarni 2000), and the fact that the pulsed fraction of optical light is significantly greater than it is in X-rays, ruling out reprocessing of X-rays in a disc as its origin (Kern & Martin 2002; but see Ertan & Cheng 2004). Both of these optical constraints have been obtained via observations of the brightest known AXP, 4U 0142+61. In this paper we report on new high-speed, multicolour optical observations of this object, obtained with the aim of confirming the high optical pulsed fraction observed by Kern & Martin (2002).

2 OBSERVATIONS AND DATA REDUCTION

The observations of 4U 0142+61 presented in this paper were obtained with ULTRACAM (Dhillon & Marsh 2001; Beard et al. 2002) at the Cassegrain focus of the 4.2-m William Herschel Telescope (WHT) on La Palma. ULTRACAM is a charge-coupled device (CCD) camera designed to provide imaging photometry at high temporal resolution in three different colours simultaneously. The instrument provides a 5 arcmin field on its three 1024×1024 E2V 47-20 CCDs (i.e. 0.3 arcsec pixel^{-1}). Incident light is first collimated and then split into three different beams using a pair of dichroic beam splitters. For the observations presented here, one beam was dedicated to the SDSS u' (3543 Å) filter, another to the SDSS g' (4770 Å) filter and the third to the SDSS i' (7625 Å) filter. Because ULTRACAM employs frame-transfer chips, the dead-time between exposures is negligible: we used ULTRACAM in its two-windowed mode, each of 100×200 pixels, resulting in an exposure time of 0.48 s and a dead-time of 0.025 s. A total of 30 618 and 31 304 frames of 4U 0142+61 were obtained on the nights of 2002 September 10 and 12, respectively, with each frame time-stamped to a relative accuracy of better than 50 μs using a dedicated GPS system.[1] Both sets of data were obtained in photometric conditions, with no Moon and i'-band seeing of 0.75 and 0.65 arcsec on 2002 September 10 and 12, respectively.

A portion of the summed i' image from the night of September 12 is shown in Fig. 1. The vertical streaks are due to light from bright stars falling on the active area of the chip above the CCD windows. The data we obtained on September 10 (not shown in Fig. 1) suffer from streaks passing through the position of 4U 0142+61, increasing the background noise level significantly. As a result, we rotated the Cassegrain rotator in advance of our observations on September 12 so that no streaks passed through 4U 0142+61. For this reason, the data obtained on September 12 are of a much higher quality than the data obtained on September 10. Note that the vertical streaking problem has since been rectified in ULTRACAM by provision of an adjustable focal-plane mask, which blocks the light from bright stars (and the sky) above the CCD windows (Stevenson 2004).

[1] The absolute timing accuracy of ULTRACAM was verified with contemporaneous observations of the Crab pulsar. Our observed time of optical pulse maximum was found to agree with the ephemeris of Lyne, Jordan & Roberts (2005) to better than 1 ms (the quoted error in the Crab pulsar ephemeris during 2002 September).

The data were reduced using the ULTRACAM pipeline software. All frames were first debiased and then flat-fielded, the latter using the median of twilight sky frames taken with the telescope spiralling. We then extracted light curves of 4U 0142+61 using two different techniques.

2.1 Technique (i)

Kern & Martin (2002) obtained their light curve of 4U 0142+61 by synchronizing the CCD clocks in their camera to the X-ray spin period of 4U 0142+61, resulting in the accumulation of 10 on-chip phase bins. This has the advantage of reducing detector noise, but the potential disadvantage that a period must be assumed before the data have been taken and, if the period is wrong, the true pulse profile is unrecoverable.

To mimic the Kern & Martin (2002) technique, we assumed a spin period for 4U 0142+61 on September 12 of 8.688 473 130 s, which was calculated from the updated X-ray ephemeris given in Table 1. Note that this ephemeris spans our WHT observations and is hence more reliable for our purposes than using the ephemeris of Gavriil & Kaspi (2002) adopted by Kern & Martin (2002). Each ULTRACAM data frame was then added to one of 10 evenly spaced phase bins covering the spin cycle of 4U 0142+61, resulting in 10 high signal-to-noise ratio data frames. An optimal photometry algorithm (Naylor 1998) was then used to extract the counts from 4U 0142+61 and a bright comparison star 24 arcsec to the east of the AXP (see Fig. 1), the latter acting as the reference for the profile fits and transparency variation correction. The position of 4U 0142+61 relative to the comparison star was determined from a sum of all the images, and this offset was then held fixed during the reduction so as to avoid aperture centroiding problems. The sky level was determined from a clipped mean of the counts in an annulus surrounding the target stars, and subtracted from the object counts.

2.2 Technique (ii)

The second approach we took to light-curve extraction was identical to that described above, except that we omitted the phase-binning step and simply performed optimal photometry on the 61 922 individual ULTRACAM data frames. In other words, we made no assumption about the spin period of 4U 0142+61.

3 RESULTS

3.1 Magnitudes

We were unable to detect 4U 0142+61 in u', at a detection limit of $u' > 25.8$. We did, however, clearly detect it in g' and i' on both nights at magnitudes of $g' = 27.2 \pm 0.2$ and $i' = 23.7 \pm 0.1$, as shown in Fig. 1. Hulleman et al. (2004) measured $g' \sim 26.9$ and $i' \sim 23.7$ (where we have converted their *BVRI* Johnson–Morgan–Cousins magnitudes to SDSS magnitudes using the transformation equations of Smith et al. 2002), indicating that 4U 0142+61 was approximately the same magnitude during our observations.

3.2 Pulse profiles

The two data reduction techniques described in Section 2 result in two different pulse profiles for 4U 0142+61.

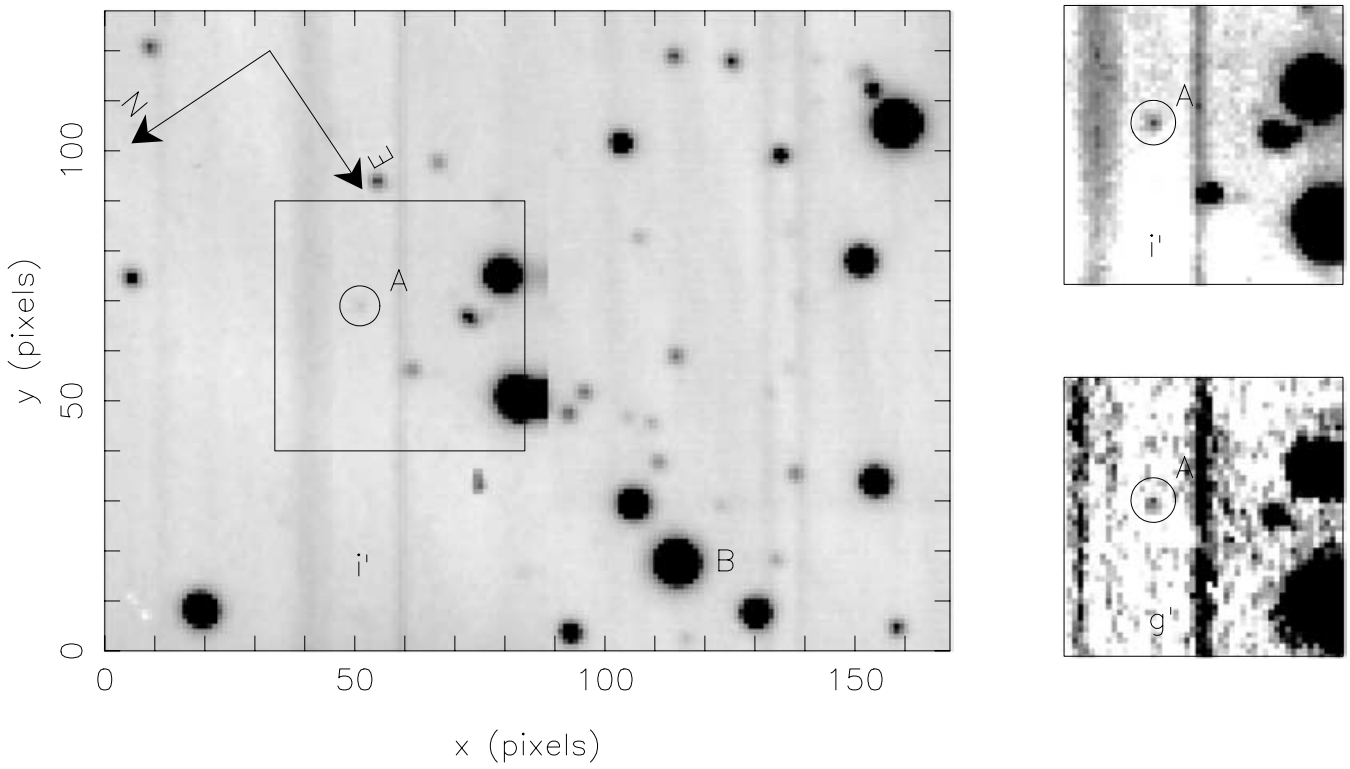

Figure 1. Left: summed i' image from the night of 2002 September 12, with a total exposure time of 15 046 s (∼4 h). Star A is 4U 0142+61 and star B is the comparison/reference star (see Hulleman et al. 2004 for coordinates and magnitudes). The orientation arrows represent 10 arcsec on the sky. For clarity, only a portion of the two ULTRACAM windows is shown. Note that there is no gap between the windows, but a faint discontinuity between them can be seen running down the centre of the image, due to the fact that each window is read out via a separate channel. Right: higher-contrast plots of the field around 4U 0142+61 (star A), showing the summed i' (top) and g' images (bottom) from the night of September 12. The box in the left-hand image shows the portion of the field shown (at the same scale) in the right-hand images.

Table 1. Updated ephemeris for 4U 0142+61 spanning the optical observations described in Section 2, based on the monitoring campaign described in Gavriil & Kaspi (2002). BMJD refers to the Barycentric-corrected Modified Julian Date on the Barycentric Dynamical Timescale (TDB). TOA refers to the pulse time of arrival (see Gavriil & Kaspi 2002 for details). The errors on the last two digits of each parameter are given in parentheses.

BMJD range	51 610.636–53 401.184
TOA arrival points	79
ν (Hz)	0.115 095 074 45(18)
$\dot{\nu}$ (10^{-14} Hz s^{-1})	−2.664 78(36)
$\ddot{\nu}$ (10^{-24} Hz s^{-2})	5.08(23)
Epoch (BMJD)	52 506.974 887 427 4228
rms residual (cycles)	0.031

3.2.1 Technique (i)

The first technique produced the pulse profiles shown in the top panel of Fig. 2. As expected, the light curve of September 12 is of a significantly higher quality than that of September 10, but both show approximately the same morphology as the optical pulse profile presented by Kern & Martin (2002), exhibiting a broad (arguably double-humped) structure with peaks around phases 0.65 and 1.15 and a minimum around phase 0.35. These phases are different from the corresponding phases in the pulse profile of Kern & Martin (2002), but this is to be expected given that, as discussed by Kern & Martin (2002), their optical observations were obtained outside the span of the ephemeris they used and the source does exhibit some timing noise (Gavriil & Kaspi 2002). Our timing solution, on the other hand, is based on the updated ephemeris for 4U 0142+61 presented in Table 1, which spans our WHT observations and is hence reliable.

There is some similarity in the morphologies of the optical pulse profile shown in the top panel of Fig. 2 and the 2–10 keV X-ray pulse profile shown below it, where the latter is an updated version of the data presented by Gavriil & Kaspi (2002). Both profiles share a similar broad/double-humped morphology. Moreover, since the X-ray light curve shown in Fig. 2 has also been phased using the ephemeris given in Table 1, it can be seen that the optical and X-ray pulse profiles are approximately in phase with each other. To quantify this, the optical pulse profile was cross-correlated with the X-ray pulse profile. The resulting peak in the cross-correlation function was fitted with a parabola to derive a shift of 0.04 ± 0.02 cycles (i.e. 0.35 ± 0.17 s), where a positive phaseshift implies that the optical pulse profile lags the X-ray pulse profile. This result is only marginally significant (at the 2σ level) owing to the low signal-to-noise ratio and time resolution of the optical data, and additional data will be required in order to confirm that the phaseshift is significantly different from zero (discounting the unlikely situation in which the time delay is approximately equal to some multiple of the spin period).

The modulation amplitude of the pulses presented in Fig. 2 can be measured using a peak-to-trough pulsed fraction, $h_{\rm pt}$, defined as

$$h_{\rm pt} = \frac{F_{\rm max} - F_{\rm min}}{F_{\rm max} + F_{\rm min}}, \quad (1)$$

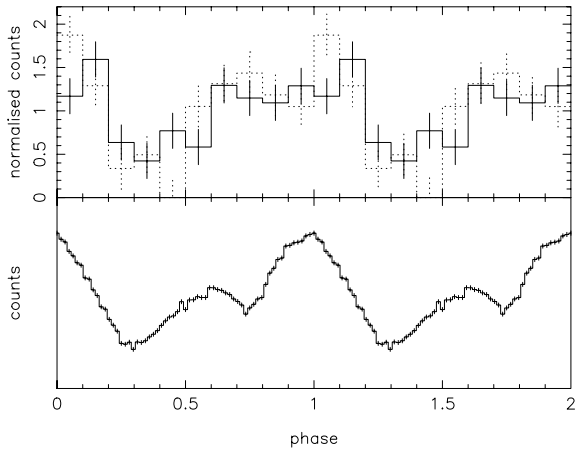

Figure 2. Top: pulse profiles of 4U 0142+61 in the i' band on 2002 September 12 (solid line), obtained using technique (i) (Section 2.1). The dotted line shows the poorer-quality light curve we obtained on the night of 2002 September 10, demonstrating the repeatability of the pulse profile. Each pulse profile was first corrected for transparency variations using the comparison star (star B in Fig. 1), although the correction made only a negligible difference to the light curves. The pulse profiles were then normalized by dividing by the mean number of counts. Note that the formal error bars on these pulse profiles were unreliable (most probably due to the vertical streaks shown in Fig. 1), and hence the error bars shown have been calculated from the scatter in the light curve extracted using technique (ii) (Section 2.2). Bottom: averaged X-ray pulse profile of 4U 0142+61 in the 2–10 keV energy band, which is an updated version of the profile presented in Gavriil & Kaspi (2002). Note that it is not possible to estimate the X-ray pulsed fraction from this profile, as the background level (i.e. the minimum flux) in the X-ray pulse profile is unrelated to the pulsar (see Section 4 for details). For this reason, no scale is given on the ordinate.

where $F_{\rm max}$ and $F_{\rm min}$ are the maximum and minimum flux in the pulse profile, respectively. We find a value of $h_{\rm pt} = 58 \pm 16$ per cent on September 12, higher than the pulsed fraction of $h_{\rm pt} = 27 \pm 8$ per cent derived by Kern & Martin (2002), although the difference between the two values is only marginally significant (31 ± 18 per cent, i.e. $<2\sigma$). There are a number of factors that might contribute to a higher optical pulsed fraction in our data, as follows.

(i) The pulsed fraction measured from our data refers to the i' band, whereas that of Kern & Martin (2002) is for white light (4000–10 000 Å). If the optical pulsed fraction varies with wavelength, this could be the source of the discrepancy. Note that, unfortunately, our g' data were too faint to extract a pulse profile from, so we are not in a position to test this explanation.

(ii) Even a small error in the assumed period on which the data is phase-binned can result in a smearing of the pulse profile and hence a reduction in the measured pulsed fraction. We have simulated this effect and find that, to reduce our pulsed fraction to the level observed by Kern & Martin (2002), the period must be in error by greater than ∼0.003 s. This is three orders of magnitude greater than the timing accuracy achieved by the instrumentation used by Kern & Martin (2002) and hence an error in the period used to phase-bin the data is an unlikely source of the discrepant pulsed fractions.

(iii) The higher pulsed fraction in our data might be due either to a decrease in the unpulsed optical component or to an increase in the pulsed optical component. Hulleman et al. (2004) found no evidence for long-term R-band variability in 4U 0142+61, down to a 2σ limit of 0.09 mag, and our magnitude estimates (Section 3.1) appear to support this conclusion. Note, however, that Hulleman et al. (2004) did find long-term variability of ∼0.5 mag in their K-band observations of 4U 0142+61, which they tentatively attributed to the occurrence of SGR-like bursts in 4U 0142+61. X-ray observations of this source have not shown such bursts, but this might be due to their (expected) low amplitude and the efficiency of the X-ray monitoring.

(iv) The peak-to-trough pulsed fraction defined in equation (1) effectively adds any noise present in the light curve to the true pulsed fraction, thereby tending to increase the resulting measurement. A more robust estimate is given by the rms pulsed fraction, $h_{\rm rms}$, defined as

$$h_{\rm rms} = \frac{1}{\bar{y}} \left[\frac{1}{n} \sum_{i=1}^{n} (y_i - \bar{y})^2 - \sigma_i^2 \right]^{1/2}, \qquad (2)$$

where n is the number of phase bins per cycle, y_i is the number of counts in the ith phase bin, σ_i is the error on y_i and $\bar{y}$ is the mean number of counts in the cycle. As expected, measuring the optical pulsed fraction in this way gives a lower value of $h_{\rm rms} = 29 \pm 8$ per cent. This is much closer to the value derived by Kern & Martin (2002), but it should be stressed that these authors measured the peak-to-trough pulsed fraction (equation 1), not the rms pulsed fraction (equation 2).

(v) The higher pulsed fraction in our data could be due to some systematic problem with the sky subtraction. We consider this to be unlikely, however, as one would not then expect our magnitude estimates to agree with those of Hulleman et al. (2004).

3.2.2 Technique (ii)

The second data reduction technique (Section 2.2) can be used to provide a check on the reliability of the optical pulse profile shown in Fig. 2. To do this, it is first necessary to fold the extracted light curve on the pulse period. Rather than do this by adopting the X-ray ephemeris given in Table 1, as we did in Fig. 2, we can instead determine the pulse period directly from our optical data using a periodogram and then fold the data on this period.

Fig. 3 shows the Lomb–Scargle periodograms (Press & Rybicki 1989) for the 30 618 and 31 304 points in the i' light curves

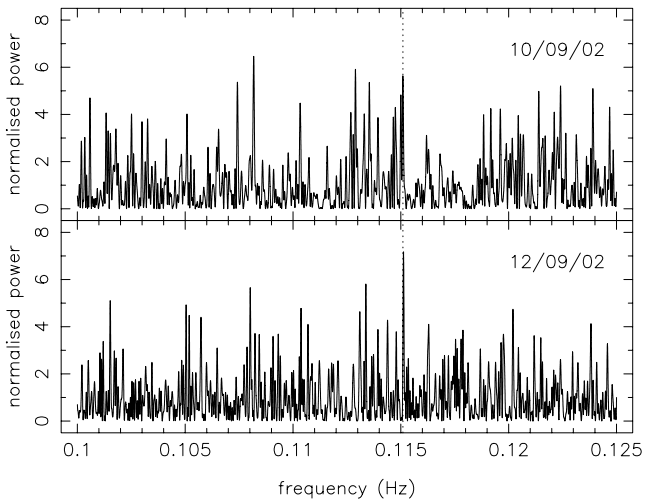

Figure 3. Lomb–Scargle periodograms of 4U 0142+61 in the i' band on 2002 September 10 (top panel) and September 12 (bottom panel), obtained using the light curves from technique (ii) (Section 2.2). The dotted line shows the predicted X-ray pulse frequency of 0.115 095 021 30 Hz on September 12, calculated from the ephemeris given in Table 1.

obtained on September 10 and 12, respectively. The g' light curves were unfortunately too noisy to perform such an analysis. The light curves were first corrected for transparency variations and then detrended by subtracting their mean level. The highest peak in the resulting periodogram of September 12 occurs at a period of 8.687 ± 0.002 s, where the error is given by the width (σ) of a Gaussian fit to the peak in the periodogram. This period is consistent with the X-ray pulse period given in Table 1. Although noisier, an equivalent peak is also present in the periodogram of September 10, with a period of 8.688 ± 0.002 s, thereby confirming that we have indeed detected the X-ray pulsation of 4U 0142+61 in the optical. We further tested the robustness of our period detection by constructing 10 000 randomized light curves from the original light curves by randomly reordering the y-axis points. Only 0.12 per cent of the resulting 10 000 periodograms for the September 12 data set showed a higher peak at 8.687 s, and only 0.38 per cent showed a higher peak at 8.688 s in the September 10 data set.

Folding the i' light curve of September 12 on the derived optical pulse period of 8.687 s gives the pulse profile shown in Fig. 4. The same data folded on the X-ray pulse period of 8.688 473 130 s is shown for comparison. Note that the phasing of both profiles can be directly compared to that in Fig. 4, as all of the data were folded using the zero point given in Table 1.

As one would expect, the i' data folded on the X-ray pulse period (dotted line in Fig. 4) is in excellent agreement with that presented in Fig. 2, in terms of morphology, phasing and pulsed fraction ($h_{\rm pt} = 50 \pm 20$ per cent). The i' data folded on the optically determined pulse period (solid line in Fig. 4) shares approximately the same phase of pulse maximum and pulsed fraction ($h_{\rm pt} = 56 \pm 16$ per cent), but the morphology is slightly different. In particular, the shape and phase of pulse minimum are very different. This is to be expected, however, given that the data have been folded on the optically derived period of 8.687 s, which is much less accurate than the X-ray period owing to the lower quality of the optical data.

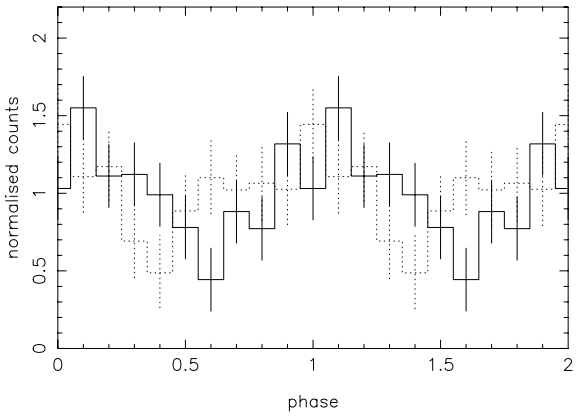

Figure 4. Pulse profiles of 4U 0142+61 in the i' band on 2002 September 12, obtained using technique (ii) (Section 2.2) and folding the resulting data on the optically determined period of 8.687 s (solid line) and on the X-ray period of 8.688 473 130 s (dotted line). The data were first corrected for transparency variations using the comparison star (star B in Fig. 1). The pulse profiles were then normalized by dividing by the mean number of counts. Note that the formal error bars on these pulse profiles were unreliable (most probably due to the vertical streaks shown in Fig. 1), and hence the error bars shown have been calculated from the scatter in the unfolded light curve.

4 DISCUSSION AND CONCLUSIONS

Using two different data reduction techniques we have shown that the optical light from 4U 0142+61 pulsates on the X-ray period, thereby confirming the discovery of Kern & Martin (2002). The morphologies of the 2–10 keV and i' pulse profiles are quite similar, both exhibiting a broad/double-humped structure. The optical lags the X-rays by only 0.04 ± 0.02 cycles (0.35 ± 0.17 s), i.e. there is no strong evidence for a phase-shift between the two pulse profiles. The most reliable value we have derived for the optical pulsed fraction is $h_{\rm rms} = 29 \pm 8$ per cent, as this is the more robust rms figure (as opposed to the peak-to-trough value) and has been obtained by folding the best data set, that of September 12, on the accurately known X-ray period (see Fig. 1). The X-ray pulsed fraction of 4U 0142+61 cannot be measured from the X-ray pulse profile shown in Fig. 2, unfortunately, as the background level (i.e. the minimum flux) in these data is unrelated to the pulsar. This is because the X-ray data were obtained with the Proportional Counter Array (PCA) on the *Rossi X-ray Timing Explorer* (*RXTE*), which has approximately a 1° field of view and no imaging capability. Instead, we turn to the work of Patel et al. (2003), who reported X-ray pulsed fractions for 4U 0142+61 of $h_{\rm rms} = 4.6 \pm 0.5$ per cent between 0.2 and 1.3 keV, $h_{\rm rms} = 4.1 \pm 0.4$ per cent between 1.3 and 3.0 keV, and $h_{\rm rms} = 5.6 \pm 1.0$ per cent between 3.0 and 8.0 keV; Patel et al. (2003) also quote corresponding peak-to-trough pulsed fractions of $h_{\rm pt} = 8.4 \pm 1.6$ per cent, $h_{\rm pt} = 7.4 \pm 1.2$ per cent and $h_{\rm pt} = 11.7 \pm 3.2$ per cent. These values demonstrate that the optical rms pulsed fraction we have measured is 5–7 times greater than the X-ray rms pulsed fractions, consistent with the factor of 5–10 times derived by Kern & Martin (2002) from their peak-to-trough pulsed fraction measurements.

We have measured g' and i' magnitudes consistent with the *BVRI* magnitudes found by Hulleman et al. (2004), supporting their finding that, although variable in the infrared and X-rays, 4U 0142+61 does not appear to show long-term variability in the optical part of the spectrum. Moreover, the fact that we have used the *B* and *V* magnitudes of Hulleman et al. (2004) to derive a g' magnitude consistent with our own confirms that the spectral break between *B* and *V* found by Hulleman et al. (2004) is real.

The optical observations presented in this paper therefore lend additional weight to the arguments given by Hulleman et al. (2000), Kern & Martin (2002) and Hulleman et al. (2004) that the AXPs are best explained by the magnetar model, mainly thanks to the failure of most alternative models to explain the observations [a notable exception is the disc–star dynamo gap model of Ertan & Cheng (2004)]. In particular, fall-back accretion disc models (e.g. Perna, Hernquist & Narayan 2000) fail because the optical flux is assumed to be due to reprocessing of the X-ray flux in the disc and therefore would not be expected to show either an optical pulsed fraction significantly in excess of the X-ray pulsed fraction (see Kern & Martin 2002) or a non-thermal spectral energy distribution in the optical. In addition, such reprocessing might also be expected to result in the optical pulses lagging the X-ray pulses in phase by an amount depending on the light travel-time to the reprocessing structure, the reprocessing time-scale within it and its location with respect to the X-ray source and Earth. We have shown that there is no strong evidence for a phaseshift between the optical and X-ray pulses, lending further evidence in support of the magnetar model.

ACKNOWLEDGMENTS

We thank the referee for valuable comments on the original manuscript. TRM acknowledges the support of a PPARC Senior Research Fellowship. SPL is supported by PPARC grant PPA/G/S/2003/00058. ULTRACAM is supported by PPARC grant PPA/G/S/2002/00092. The William Herschel Telescope is operated on the island of La Palma by the Isaac Newton Group in the Spanish Observatorio del Roque de los Muchachos of the Instituto de Astrofísica de Canarias.

REFERENCES

Beard S. M., Vick A. J. A., Atkinson D., Dhillon V. S., Marsh T. R., McLay S., Stevenson M. J., Tierney C., 2002, in Lewis H., ed., Proc. SPIE Vol. 4848, Advanced Telescope and Instrumentation Control Software II. SPIE, Bellingham, WA, p. 218
Dhillon V., Marsh T., 2001, New Astron. Rev., 45, 91
Ertan Ü., Cheng K. S., 2004, ApJ, 605, 840
Gavriil F. P., Kaspi V. M., 2002, ApJ, 567, 1067
Gavriil F. P., Kaspi V. M., Woods P. M., 2002, Nat, 419, 142
Hulleman F., van Kerkwijk M. H., Kulkarni S. R., 2000, Nat, 408, 689
Hulleman F., van Kerkwijk M. H., Kulkarni S. R., 2004, A&A, 416, 1037
Israel G. L., Mereghetti S., Stella L., 2002, Mem. Soc. Astron. Ital., 73, 465
Kaspi V. M., Gavriil F. P., Woods P. M., Jensen J. B., Roberts M. S. E., Chakrabarty D., 2003, ApJ, 588, L93
Kern B., Martin C., 2002, Nat, 417, 527
Lyne A. G., Jordan C. A., Roberts M. E., 2005, Monthly Ephemeris, Jodrell Bank Crab Pulsar Timing Results. Jodrell Bank Observatory, Univ. Manchester
Mereghetti S., Chiarlone L., Israel G. L., Stella L., 2002, in Becker W., Lesch H., Trümper J., eds, MPE Report 278, Neutron Stars, Pulsars, and Supernova Remnants. MPE, Garching, p. 29
Naylor T., 1998, MNRAS, 296, 339
Patel S. K. et al., 2003, ApJ, 587, 367
Perna R., Hernquist L., Narayan R., 2000, ApJ, 541, 344
Press W. H., Rybicki G. B., 1989, ApJ, 338, 277
Smith J. A. et al., 2002, AJ, 123, 2121
Stevenson M. J., 2004, PhD thesis, Univ. Sheffield
Thompson C., Duncan R. C., 1996, ApJ, 473, 322
Thompson C., Lyutikov M., Kulkarni S. R., 2002, ApJ, 574, 332
Woods P. M., Thompson C., 2005, in Lewin W. H. G., van der Klis M., eds, Compact Stellar X-ray Sources. Cambridge Univ. Press, Cambridge, in press (astro-ph/0406133)

This paper has been typeset from a TEX/LATEX file prepared by the author.